

A 3D Eulerian-Lagrangian Numerical Model for Sediment Transport

Berend van Wachem*, Xiao Yu[†] and Tian-Jian Hsu[†]

* Department of Mechanical Engineering, Imperial College London, Exhibition Road, London, SW7 2AZ

[†] Civil and Environmental Engineering, University of Delaware, Newark, DE 19716, USA

b.van-wachem@imperial.ac.uk and thsu@udel.edu

Keywords: Lagrangian simulations, Sedimentation Transport

Abstract

In this study, a new approach for sediment transport utilizing 3D turbulence resolving Eulerian-Lagrangian framework is presented. The model employs slightly modified Navier-Stokes equations to determine the motion of the fluid phase. The motion of the sediment phase is elucidated by a Lagrangian or Discrete Element Method (DEM), implying that the individual trajectory of each particle is determined by approximating Newton's second law of motion. The forces acting on each particle are gravity, the traction force of the fluid phase, and the force resulting from the interaction with other particles. The traction force of the fluid phase is determined by an empirical equation which has been validated for low particle Reynolds numbers. The total effect of the traction force summed over all particles is exactly opposite to the inter-phase momentum transfer added to the fluid-phase momentum equations. The force accounting for inter-particle collisions is based upon a so-called "soft-sphere" approach, following Tsuji (1994), which estimates the force based upon the deformation of each particle resulting from the interaction with other particles. We have performed simulation of sediment transport a 3 dimensional domain of approximately 50x30x50 particle diameters. The two directions perpendicular to gravity are treated as periodic; i.e. the domain is fictitiously extended to infinity in those directions. The flow is driven by an external pressure drop that corresponds to Shields parameter around 1.1. Next to the Eulerian-Lagrangian simulations, turbulence-averaged 1DV Eulerian-Eulerian simulations based upon the kinetic theory of granular flow are performed as well. The 3D model results are compared and the results from the Eulerian-Lagrangian simulations are analyzed to obtain flow statistics, which can be used as a starting point for Eulerian-Eulerian closure model validation and development.

Introduction

The phenomena of sediment transport is defined as the movement of solid particles due to a combination of gravity acting on the particles (i.e. the sediment), the intra-particle forces, and the movement of the fluid in which the sediment is entrained. Sediment transport due to fluid motion occurs in rivers, the oceans, lakes, due to currents, waves, and tides. Sediment transport in water involves complicated fluid-particle interactions and inter-granular interactions. A comprehensive description of various mode of sediment transport, namely, bedload and suspended load, requires a multi-phase flow approach. Existing modeling approach for sediment transport utilize Reynolds-averaged approach in the Eulerian-Eulerian framework (Dong and Zhang 2002; Hsu et al. 2004; Amoudry and Liu 2009) or Eulerian-Lagrangian framework (Drake and Calantoni 2001).

Modelling of sediment transport in rivers and coastal areas is important in identifying erosion, changes in fluvial and coastal morphology and the health of ecosystem. Models have been successfully used to study wave-induced sand transport under energetic waves, i.e., sheet flow condition (Dong and Zhang 2002; Hsu and Hanes 2004; Yu et al. 2010). Through Reynolds-averaging, these models parameterized all the scales of turbulence and related turbulence-sediment interaction. The coefficients involved in the turbulence closure hence become highly empirical. Moreover, in those models where sediment phase is modeled in an Eulerian framework, kinetic theory of granular flow is usually adopted for the closure of particle stresses. Strictly speaking, kinetic theory becomes inappropriate when sediment volume concentration becomes greater than random-loss-packing ($\approx 55\%$) and hence additional bed treatment in the regime of enduring contact

in sediment transport is also necessary.

Simulations

Fluid-phase governing equations

The equations for the fluid-phase are derived analogously to the Navier-Stokes equations. However, they include a local volume fraction (Anderson and Jackson 1967) and additional source terms accounting for the presence of particles and the driving force. The governing equations are the mass continuity and conservation of momentum, which are given by equations (1) and (2) respectively,

$$\frac{\partial(\alpha_f \rho_f)}{\partial t} + \frac{\partial(\alpha_f \rho_f v_f^i)}{\partial x^i} = 0 \quad (1)$$

and

$$\begin{aligned} \frac{\partial(\alpha_f \rho_f v_f^j)}{\partial t} + \frac{\partial(\alpha_f \rho_f v_f^j v_f^i)}{\partial x^i} &= \frac{\partial(\alpha_f \tau_f^{ij})}{\partial x^i} - \alpha_f \frac{\partial p}{\partial x^j} \\ &+ T_f v_f^j + S_f^j + \sum_{p=1}^{phases \neq f} \beta_{(f,p)} [v_f^j - v_p^j] \end{aligned} \quad (2)$$

where α_f is the local volume fraction of the fluid phase, β represents the local averaged reciprocal of the particle time-scale, or drag coefficient arising from the local behaviour of the particles, T_f represents the source term linear in the velocity field; S_f^j represent the additional source terms, which are used for driving the flow, and τ_f^{ij} the stress tensor of the fluid, given by

$$\tau_f^{ij} = \mu_f \left(\frac{\partial v^i}{\partial x^j} + \frac{\partial v^j}{\partial x^i} \right) + \delta_{ij} \left(\lambda_f - \frac{2}{3} \mu_f \right) \frac{\partial v^k}{\partial x^k} \quad (3)$$

where μ_f is the shear and λ_f represent the bulk viscosity of the fluid. As a first approach, the sub-grid scale stresses are not considered.

The simulations performed in this paper use a finite volume scheme, a second order backward Euler time discretisation and a second order accurate central scheme to approximate the advective terms in the continuity and momentum equations. The solving procedure is made parallel with the MPI libraries. During the simulations, the CFL number is kept constant at 0.4, leading to a slight variation in time-step over time.

Particle-phase governing equations

A discrete element model (DEM) proposed by Cundall and Strack (1979) is used to model the particles. The individual trajectories of the particles are determined in

the Lagrangian framework, where particle collisions are modelled via the soft-sphere model proposed by Tsuji et al. (1991b), which accounts for some non-reversible deformation.

The interactions of particles with other particles and walls are dynamic of nature. This is because the particle movements are essentially defined by the particle-particle interactions; particle-wall interactions; particle-fluid interactions and/or body forces (Kuang et al. 2008). The trajectories of individual particles are considered (i.e. described in a Lagrangian framework) and Newton's 2nd law is solved for each individual particle, accounting for the fluid-particle, particle-particle, and particle-wall interactions, and approximating the integral with the Verlet algorithm.

Newton's 2nd law for the particles is written out as

$$\begin{aligned} m_p \frac{d\mathbf{v}_p}{dt} &= \beta \frac{V_p}{\alpha_p} (\mathbf{v}_f - \mathbf{v}_p) + m_p \mathbf{g} - V_p \nabla P_f \\ &+ V_p \mathbf{S}_{drive} + \sum^N [\mathbf{F}_{pw} + \mathbf{F}_{pp}] \end{aligned} \quad (4)$$

and for the rotational momentum

$$I_p \frac{d\boldsymbol{\omega}_p}{dt} = \mathbf{T}_p \quad (5)$$

where m_p is the mass of the particle; I_p is the momentum of rotational inertia; \mathbf{T}_p the torque of the particle; $\boldsymbol{\omega}_p$ is rotational velocity; \mathbf{v}_p is the translational velocity; and β is the drag function as proposed by Wen and Yu (1966), where the reciprocal of the Eulerian fluid-particle timescale is given by

$$\beta = \frac{3}{4} C_D \frac{\alpha_p \alpha_f \rho_f |\mathbf{v}_f - \mathbf{v}_p|}{d_p} \alpha_f^{-2.65} \quad (6)$$

and C_D represents the coefficient of drag for an individual particle and α_f represents the fluid volume fraction. The right hand side terms of equation (4) are outlined in table 1.

Implementation of particle collisions

The particle-particle and particle-wall interactions as taken into account in this work are assumed to be local; *i.e.* no long-range forces are included. For establishing the nature of the interaction, each particle pair could be interrogated. However, this would lead to a scaling of the computational effort with N^2 , N being the number of particles. Instead, a particle-mesh algorithm is adopted, in which each of the particles is assigned a cell in the particle mesh based upon its

Table 1: Terms of right hand side of equation(4)

Term	Force type
$\beta \frac{V_p}{\alpha_p} (\mathbf{v}_f - \mathbf{v}_p)$	Drag force
$m_p \mathbf{g}$	Body force due to gravity
$V_p \nabla P_f$	Force due to the pressure gradient
$V_p \mathbf{S}_{drive}$	External driving force
\mathbf{F}_{pw}	Particle-wall contact force
\mathbf{F}_{pp}	Particle-particle contact force

location. Using this particle-mesh, each particle is only tested for interaction against particles located in the same or directly neighbouring particle mesh cells. Although there is some additional computational effort and a slightly more complex algorithm required for this approach, it leads to a scaling of $N \log N$ with the number of particles, making it a lot more favourable for large numbers of particles.

The particle collisions are modelled by the soft-sphere model as described by Cundall and Strack (1979). In brief, this model uses a spring-dashpot-slider arrangement to describe the particle behaviour before, during and after a collision. The damping coefficient as introduced by Tsuji et al. (1991a) accounts for the non-ideal behaviour during the collision of the particles due to irreversible plastic or visco-elastic deformation.

The normal and tangential contact forces are given by the sum of forces due to the spring and dashpot. From Hertzian contact theory the normal and tangential contact forces are,

$$\mathbf{F}_{nij} = (-k_n \delta^{\frac{3}{2}} - \eta_{nj} \mathbf{G} \cdot \mathbf{n}) \mathbf{n} \quad (7)$$

$$\mathbf{F}_{tij} = -k_t \delta_t - \eta_{tj} \mathbf{G}_{ct} \quad (8)$$

where \mathbf{G} is the velocity vector of particle i relative to particle j , \mathbf{G}_{ct} is the slit velocity vector at the contact point. The subscripts n and t represent the normal and tangential components respectively and δ is the displacement, or overlap, of particles i and j during collision. Three parameters are required by the soft-sphere model; stiffness (k), damping coefficient (η) and the coefficient of friction (μ). μ is a well known empirical quantity, stiffness and the damping coefficient must be estimated using equations

$$\eta_n = \alpha \sqrt{M k_n} \delta^{\frac{1}{4}} \quad (9)$$

$$\eta_t = \alpha \sqrt{M k_t} \delta^{\frac{1}{4}} \quad (10)$$

where $M = \frac{m_i m_j}{m_i + m_j}$; and m is the mass of the particle. Note that for wall collisions $m_w \rightarrow \infty$, hence $M =$

m_p . The relationship between α and the coefficient of restitution is well defined by Tsuji et al. (1991b). The spring constants are, based upon elastic deformation,

$$k_n = \frac{4}{3} \left(\frac{1 - \sigma_i^2}{E_i} + \frac{1 - \sigma_j^2}{E_j} \right)^{-1} \left(\frac{r_i + r_j}{r_i r_j} \right)^{-\frac{1}{2}} \quad (11)$$

$$k_t = 8 \left(\frac{2 - \sigma_i}{G_i} + \frac{2 - \sigma_j}{G_j} \right)^{-1} \left(\frac{r_i + r_j}{r_i r_j} \right)^{-\frac{1}{2}} \delta_n^{\frac{1}{2}} \quad (12)$$

where r is the radius of the particles, σ the Poisson's ratio; E the Young's modulus, G the shear modulus (given by $G = \frac{E}{2(1+\sigma)}$) and δ_n the magnitude of the deformation in the normal direction. Note as above, when a particle reaches a wall, $r_w \rightarrow \infty$, hence, $\frac{r_s + r_w}{r_s r_w} = \frac{1}{r_s}$.

Simulation Parameters

The fluid properties used in the simulations are those of water, with density $\rho = 998 \frac{kg}{m^3}$ and viscosity $\nu = 1.00 \times 10^{-3} Pa \cdot s$. The driving force of the fluid is determined by the shields parameter. The shields parameter is a dimensionless parameter that characterizes the type of sediment transport regime. The Shields parameter, i.e., the nondimensionalized bed shear stress, is given by

$$\Theta = \frac{\tau}{(\rho_s - \rho_f) g d_s} \quad (13)$$

where τ is the bed shear stress, g is the gravitational acceleration, d_s represents the particle diameter, and ρ_s and ρ_f the solids and fluid density respectively. For statistical steady flow considered in this study, the given bed shear stress can be further related to pressure drop in the streamwise direction:

$$-\frac{\partial p}{\partial x} = \frac{\tau}{h} \quad (14)$$

where h is the height of the domain. The driving force is made equal to the pressure drop, i.e.

$$S_{drive} = -\frac{\partial p}{\partial x} \quad (15)$$

And this driving force is distributed over the local fluid and particle phase weighted by the local volume fraction.

For the simulations, sand (silicon dioxide) particles were taken and assumed to have constant properties, see Table 2

Results and Discussion

Eulerian-Lagrangian Simulation Results

The simulations carried out with the Shields parameter of 1.1. The resulting magnitude of the shear stress is

Table 2: Summary of the sand particle properties used in computations.

Variable	Value	Units
d_s	200 $\cdot 10^{-6}$	m
ρ_s	2650	kg/m ³
Youngs Modulus	75 $\cdot 10^7$	Pa
Poisson ratio	0.17	-
Friction Coefficient	0.45	-
Restitution Coefficient	0.95	-

$$\tau = 3.89 \text{ Pa and the pressure gradient } \frac{\partial p}{\partial x} = 55.6 \text{ Pa.}$$

According to field observation and laboratory experiments, Shields parameter greater than 1.0 represents typical "sheet flow" condition where intense sediment transport occurs, the bed is statistically flat (no bedforms or ripples) with a concentrated layer of sediment moving near the bed. A snapshot of the numerical simulation is shown in Figure 1, where the particles are coloured by their velocity.

The simulations predict the basic characteristics of sheet flow. Sediment concentration decreases rapidly away from the bed and all the transport occurs within 2 mm near the bed. In this moving layer, the fluid velocity also increases rapidly from 2 cm/s to about 20 cm/s. Numerical model predicts the statistically-averaged fluid velocity is almost identical to that of particle velocity for relatively fine sediment in water considered here.

Eulerian-Eulerian Model Results

A Eulerian-Eulerian two-phase model for sediment transport is adopted in this study. Turbulence-averaged two-phase equations are simplified into one-dimensional-vertical (1DV) to model fully-developed sheet flow sand transport driven by a steady or oscillatory flow forcing (Hsu et al. 2004; Yu et al. 2010). The eddy viscosity and $k-\epsilon$ closure for two-phase flow are adopted for fluid Reynolds stress and turbulent suspension of sediment. Kinetic theory of granular flow of Jenkins and Savage (1983) and empirically modified closure for stress due to enduring contact are utilized for the closure of particle stress. More detailed model formulations and model applications to sediment transport can be found in Hsu et al. (2004); Yu et al. (2010).

The Eulerian-Eulerian model results compared to the the Eulerian-Lagrangian model results for the same case are shown in Figure 2 for vertical profiles of fluid velocity (solid curve in the left panel), sediment

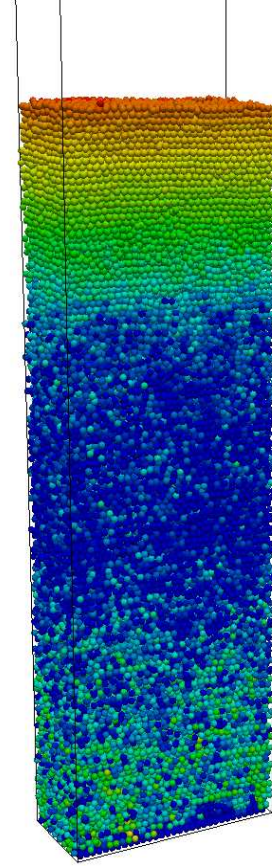


Figure 1: A snapshot of the Eulerian-Lagrangian simulations, showing the individual particles. The particles are coloured by their velocity.

concentration (solid curve in the middle panel) and fluid turbulent intensity $\sqrt{(2TKE)}$, where TKE represents the fluid turbulent kinetic energy (right panel). The fluid stress consists of turbulent Reynolds stress and viscous stress with the the viscous stress contribution negligible in this case. Eulerian-Eulerian model predicts sediment suspended much higher in the water column due to strong flow turbulence. Strong turbulence can be observed from large turbulent intensity near the bed. Some discrepancies with the Eulerian-Lagrangian model results can be observed. Most evidently, Eulerian-Eulerian model predicts more intense sediment suspension throughout the water column and higher mobility of sediment. Although it is likely that the flow turbulence and granular temperature may be over-predicted in the Eulerian-Eulerian model due to uncertainties in the closures, it is also possible that in the Eulerian-Lagrangian model, the flow turbulence is under-predicted due to low resolution used in this simulation. The under-prediction of flow turbulence can be seen from the almost linear fluid velocity profile

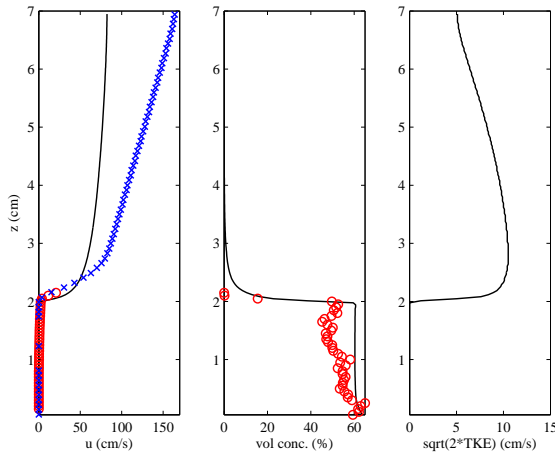


Figure 2: Eulerian-Eulerian model results(line) compared to the the Eulerian-Lagrangian model results(symbols) for the same case, for vertical profiles of fluid velocity (solid curve in the left panel), sediment concentration (solid curve in the middle panel) and fluid stress (right panel, solid curve) and particle stress (right panel, dotted curve).

away from the bed. On the other hand, Eulerian-Eulerian model also predicts almost identical fluid and sediment velocities (not shown here), consistent with Eulerian-Lagrangian model results.

Conclusions

A new approach for sediment transport utilizing 3D turbulence resolving Eulerian-Lagrangian framework is presented. Preliminary simulation results suggest the main characteristics of sheet flow in the concentrated regime of sediment transport is captured. However, higher numerical resolution for fluid phase is required, or subgrid turbulence closure need to be implemented in order to capture flow turbulence and the resulting turbulent suspension of sediment.

Acknowledgements

Financial support for Dr. Berend van Wachem's travel to ICMF-2010 is partly provided by the Royal Academy of Engineering. Financial support to Hsu and Yu is provided by U.S. National Science Foundation (OCE-0644497).

References

L.O. Amoudry and P.L.-F. Liu. Two-dimensional, two-phase granular sediment transport model with applica-

tions to scouring downstream of an apron. *Coastal Engineering*, 56:693–702, 2009.

T.B. Anderson and R. Jackson. A fluid mechanical description of fluidized beds. *Ind. Engng. Chem. Fundam.*, 6(4):527–539, 1967.

P.A. Cundall and O.D.L. Strack. A discrete numerical model for granular assemblies. *Geotechnique*, 29:47–65, 1979.

P. Dong and K. Zhang. Intense near-bed sediment motions in waves and currents. *Coastal Engineering*, 45:75–87, 2002.

T.G. Drake and J. Calantoni. Discrete particle model for sheet flow sediment transport in the nearshore. *J. Geophys. Res.*, 106:859–868, 2001.

T.-J. Hsu and D.M. Hanes. The effects of wave shape on sheet flow sediment transport. *J. Geophys. Res.*, 109:C05025, 2004.

T.-J. Hsu, J.T. Jenkins, and P. L.-F. Liu. On two-phase sediment transport: sheet flow of massive particles. *Proc. R. Soc. Lond. A*, 460:2223–2250, 2004.

J.T. Jenkins and S.B. Savage. A theory for the rapid flow of identical, smooth, nearly elastic, spherical particles. *J. Fluid Mech.*, 130:187–202, 1983.

S.B. Kuang, K.W. Chu, A.B. Yu, Z.S. Zou, and Y.Q. Feng. Computational investigation of horizontal slug flow in pneumatic conveying. *Ind. Eng. Chem. Res.*, 47:470–480, 2008.

Y. Tsuji, T. Kawaguchi, and T. Tanaka. Discrete particle simulation of two-dimensional fluidized bed. *Powder Technology*, 77:79–87, 1991a.

Y. Tsuji, T. Tanaka, and T. Ishida. Lagrangian numerical simulation of plug flow of cohesionless particles in a horizontal pipe. *Powder Technology*, 71:239–250, 1991b.

C. Y. Wen and Y. H. Yu. Mechanics of fluidization. *Chemical Engineering Progress Symposium Series*, 62:100–111, 1966.

X. Yu, T.-J. Hsu, and D.M. Hanes. Sediment transport under wave groups: Relative importance between nonlinear waveshape and nonlinear boundary layer streaming. *J. Geophysical Research*, 115:C02013, 2010.